ENVIRONMENTAL RESEARCH
LETTERS

ACCEPTED MANUSCRIPT • OPEN ACCESS

Future increases in soil moisture drought frequency at UK monitoring sites: merging the JULES land model with observations and convection-permitting UK Climate Projections

To cite this article before publication: Magdalena Szczykulska *et al* 2024 *Environ. Res. Lett.* in press https://doi.org/10.1088/1748-9326/ad7045

IOP Publishing Journal Title
Journal **XX** (XXXX) XXXXXX https://doi.org/XXXX/XXXX

Future increases in soil moisture drought frequency at UK monitoring sites: merging the JULES land model with observations and convection-permitting UK Climate Projections

Magdalena Szczykulska, Chris Huntingford, Elizabeth Cooper and Jonathan G. Evans

UK Centre for Ecology & Hydrology, Wallingford, Oxfordshire, OX10 8BB, UK

Correspondence: magszc@ceh.ac.uk

Received xxxxxx
Accepted for publication xxxxxx
Published xxxxxx

Abstract

Concerns exist about the viability of food security across Europe due to multiple, potentially adverse drivers. These include economic, political and climate forcing factors, all of which require quantification. Here, we focus on the climate forcing, and in particular, the soil moisture change component which crucially determines water availability for crop uptake. We estimate future soil moisture levels at 34 sites of the UK COsmic-ray Soil Moisture Observing System (COSMOS-UK) network. We do this by combining three platforms: the Joint UK Land Environment Simulator (JULES) land surface model, field-scale soil moisture observations from the COSMOS-UK stations and 2.2 km convection-permitting UK Climate Projections (UKCP18). We use COSMOS-UK data to optimise key soil moisture-related parameters in the JULES model, based on its performance in the contemporary period. We then force the calibrated model with UKCP18 data to produce future soil moisture estimates. We evaluate the modelled soil moisture for an average soil depth between 0 and 35 cm to match the depth of soil moisture observations. Our main conclusions concern future soil moisture droughts which we compare with equivalent events in the historical period, 1982-2000. We find that on average across all sites, there is an increase in the frequency of future extreme soil moisture drought events of duration above 90 days. In 2062-2080, such frequency increase of between 0.1 and 0.6 events per year (equivalent to at least 2 and up to 12 additional events in a 20-year period) is expected. We also show that, in 2062-2080, there is an increased risk of high or more intense soil moisture drought conditions in months between May and November, with months between June and October being at especially high risk. The UKCP18 data corresponds to a high-emissions future described by the RCP8.5 scenario.

Keywords: Soil Moisture, Climate Change, Convection-Permitting, Food Security, Data Assimilation, Soil Moisture Droughts, Cosmic-Ray Neutron Sensing

1. Introduction

Recent years have seen hotter and drier summer periods in the UK **(Met Office 2022; Turner *et al* 2021)**. Prolonged periods of reduced rainfall and increased evaporative demand can lead to exceptional drying of soils. Such drying happened, for instance, in the summer of 2022 as recorded at the UK COsmic-ray Soil Moisture Observing System (COSMOS-UK) network sites **(UKCEH 2022)**. These types of events limit the available water a plant can access via roots impacting its growth and development **(Gavrilescu 2021)**. Very dry conditions may therefore cause soil moisture droughts **(Dai 2011)** posing risks to agricultural yields and raising concerns about future food security **(Scott 2022)**. Water resource management must account for this, should more water be required for agricultural needs or new adaptation strategies be considered.

As atmospheric Greenhouse Gases (GHGs) rise, climate will change, and further intensification of hot and dry

summers is expected in the UK **(Christidis *et al* 2020; Hanlon *et al* 2021)**. The 2018 UK Climate Projections (UKCP18) provide a mechanism to assess future climate in the UK at global (60 km), regional (12 km) and local (2.2 km) spatial scales **(Kendon *et al* 2019; Lowe *et al* 2018)**. The latest 2.2 km projections offer a step change in climate prediction capability as they include local representations of the convective storm processes **(Kendon *et al* 2021)**. Hence, they capture features of rainfall patterns, storms and their intensity and duration **(Chen *et al* 2021; Kendon *et al* 2017; Kent *et al* 2022)**. Changes in rainfall characteristics may strongly influence soil moisture profiles, which in turn may impact crop growth.

There already exist studies concerning future soil moisture predictions in the UK. Work presented in **Kay *et al* (2022)** uses a 1 km grid hydrological model forced by regional UKCP18 data to predict future soil moisture across the UK. It finds significant increases in the spatial occurrence of low soil moisture levels, along with later soil wetting dates. **Rudd *et al* (2019)** also use a grid-based hydrological model forced by a large ensemble of regional climate projections for the UK obtained from the weather@home2 system. The results show increased severity of soil moisture droughts in the future. The report of **Kendon *et al* (2019)** uses directly the local (and regional) UKCP18 data to drive the Joint UK Land Environment Simulator (JULES) land surface model for soil moisture estimation. Its findings point to increased future soil moisture stress, especially in the South East of England, with September being the driest month.

On the broader spatial scale, **Grillakis (2019)** uses a soil moisture index (SMI) to show increased severity of future soil moisture droughts in Europe. **Samaniego *et al* (2018)** use a multi-model climate ensemble to drive two hydrological and two land surface models for soil moisture drought evaluation. The authors find that an increase in the global mean temperature from 1.5 K to 3 K increases the drought area by 40% (±24%) in Europe.

The above studies look at soil moisture averaged over a depth of 1 m or, in the case of **Kay *et al* (2022)** and **Rudd *et al* (2019)**, over a soil column which depth can vary from a few centimetres to several metres. They typically use regional or global climate data except for the report of **Kendon *et al* (2019)** which uses convection-permitting model (CPM) UKCP18 data. Although these works provide valuable new understanding, critically, none of them use available soil moisture observations to calibrate and assess the underlying hydrological or land surface model.

In **E. Cooper *et al* (2021)**, field-scale soil moisture observations from 16 sites of the COSMOS-UK network **(H. M. Cooper *et al* 2021)** are assimilated into the JULES model. Here, we combine this approach, of calibrating the JULES model against COSMOS-UK data, with CPM projections to generate better constrained future soil moisture estimates.

Specifically,

- We estimate soil moisture at 34 COSMOS-UK sites in three time periods: 1982-2000, 2022-2040 and 2062-2080, with future periods following the RCP8.5 high-emissions scenario. We do this by merging the JULES land surface model, COSMOS-UK field-scale soil moisture observations and the 2.2 km CPM UKCP18 data.

- We investigate the implications for soil moisture droughts by looking at the frequency of the drought events and how they affect individual months.

We evaluate the modelled soil moisture for an average value over a depth between 0 and 35 cm as guided by the COSMOS-UK observation depth. Although rooting zones of some UK crops can reach one metre or more, most, such as wheat, oat and barley, have majority of their roots in the upper 30 cm **(Fan *et al* 2016)**. Knowledge of moisture in the topmost layers of soil is especially relevant in the early plant growth stages when all roots occupy shallower depths.

2. Methods

2.1 COSMOS-UK observations

COSMOS-UK is the UK's state-of-the-art in situ soil moisture monitoring network **(H. M. Cooper *et al* 2021; Evans *et al* 2016)**. Since its start in 2013, it has established 51 observation stations spread across the UK, with the majority located in the South.

The primary product measured at the sites is soil moisture obtained using the Cosmic-Ray Neutron Sensing (CRNS) method **(Zreda *et al* 2012)**. The measurement has a horizontal footprint of approximately 12 Ha and a vertical footprint between 20 and 30 cm. The exact values of these footprints vary with soil moisture **(Köhli *et al* 2015)**. Averaging spatially over micro-scale soil moisture heterogeneity (for instance macropores which are not represented in JULES) is the key benefit of using this measurement, over point sensors, for calibrating the JULES model for soil moisture estimation.

Associated with this measurement technique is statistical noise, which we suppress by using a longer time-average, daily soil moisture product. Alongside soil moisture, half-hourly meteorological variables necessary for driving the JULES model are also recorded at the COSMOS-UK sites **(Table 1)**.

Variable	**Units**
Precipitation	kg m^{-2} s^{-1}
Temperature	K
Downward shortwave radiation	W m^{-2}
Downward longwave radiation	W m^{-2}
Specific humidity	kg kg^{-1}
Wind speed	m s^{-1}
Pressure	Pa

Table 1. Meteorological variables and their units required for driving the JULES land model.

2.1.1 COSMOS-UK site selection

We calibrate the JULES model at 26 sites using soil moisture observations from one selected full year at each location (one site-year). The site-year selection **(Suppl. Section S1.1)** is mostly based on strict completeness criteria for precipitation data, recognising its importance as a primary driver of soil moisture variations. We also avoid peatland sites, as our modelling methodology is designed for mineral soils, and woodland sites, as CRNS soil moisture estimates are known to be less accurate there.

The future predictions of soil moisture are then performed at 34 sites: 25 calibration sites and nine extra (non-calibration) sites of direct prediction. For the non-calibration sites, we select the remaining non-peatland and non-woodland sites. We also exclude one of the calibration sites (hence leaving 25) due to the presence of particularly large biases there when assessing the model **(Section 2.3.1)**. **Figure 1** shows a map of the full set of 35 sites and **Suppl. Section S1.2** explains their vegetation characteristics.

Figure 1. Map of COSMOS-UK sites used in this study. Each location is marked with the standard COSMOS-UK identifying site code. The places of calibration (also used for forward projections) are marked as blue dots and sites of forward projections only as green dots. The site labelled in red is used for calibration, but not forward projections due to the presence of large soil moisture biases in the modelled data **(Section 2.3.1)**.

2.2 The JULES Land Surface Model

The JULES model simulates physical land surface processes and quantities, including soil moisture **(Best *et al* 2011)**. The model solves the Darcy-Richards equation to represent water movement between four soil layers: 0-10 cm, 10-35 cm, 35-100 cm and 100-300 cm. The amount of water retained in the layers depends on soil hydraulic characteristics which are related to easier-to-measure soil properties, such as soil texture, via pedotransfer functions (PTFs) **(Van Looy *et al* 2017)**. A well calibrated set of PTFs ensures a better representation of the physical processes necessary for soil moisture estimation.

We run the JULES standalone model, for 1D simulations, in a configuration described in **Cooper *et al* (2022)** which closely matches the RAL3M configuration, a recent update on the Regional Atmosphere and Land configuration RAL1 **(Bush *et al* 2020)**. We source soil textures for the selected COSMOS-UK sites from the Harmonized World Soil Database (HWSD) **(Fischer *et al* 2008)**. These soil textures are considered constant over the entire 300 cm depth.

2.3 Calibration of the JULES model with COSMOS-UK observations

We use methodology from **E. Cooper *et al* (2021)** to optimise 12 parameters of Cosby PTFs using the COSMOS-UK soil moisture observations, thereby improving JULES soil moisture outputs. The PTF parameters are common to all studied soil types. We use the LaVEnDAR four-dimensional ensemble variational data assimilation framework **(Pinnington *et al* 2021; Pinnington *et al* 2020)** which here minimises a cost function with two terms: the difference between the modelled and observed soil moisture, and the difference between prior and posterior values of the 12 PTF parameters. These two terms are weighted by their corresponding errors: observation error and that of the prior PTF parameters respectively. The method therefore considers both prior parameter and observational uncertainties and combines them within the cost function. Here, we assume a 10% error on the prior PTF parameters and inflated uncorrelated observation errors of 50% of the mean soil moisture value at each site as described in **E. Cooper *et al* (2021)**. The high observation error includes contributions from instrument error and, crucially, representativity error between the modelled and measured soil moisture **(Waller *et al* 2018)**.

To produce the modelled soil moisture for the PTF parameter optimisation, we first perform a model spin-up at each of the 26 selected sites for one year preceding the

calibration year **(Suppl. Table S1)**. We repeat the spin-up process twice so that it is equivalent to three years of spin-up. Here, we use the hourly ERA5-Land data **(Muñoz Sabater 2019)** for all driving variables listed in **Table 1** due to the incompleteness of the COSMOS-UK observations for the required sites and years. We convert the hourly ERA5-Land drivers to half-hourly values to match the temporal resolution used in our main simulations. We note that either hourly or half-hourly resolutions would be suitable given that we use daily mean soil moisture values in our analysis. We move from the spin-up period to the simulation period on 1st January when soil is likely close to saturation, which reduces the effect of any biases between the driving meteorology.

We then force the JULES model with the half-hourly COSMOS-UK observations **(Table 1)**, for the selected calibration year at each site, to estimate soil moisture at four depth layers listed in **Section 2.2**. For comparison with observations, we apply depth weightings to the different modelled soil moisture layers to correspond to the measurement depth **(Suppl. Section S1.4)**. We then input the resulting modelled daily soil moisture, alongside soil moisture observations and the prior PTF parameters, into the data assimilation algorithm to produce a single posterior set of PTF parameters which we later also use for non-calibration sites. Details of COSMOS-UK and ERA5-Land data processing are given in **Suppl. Section S1.3**. **Figure 2 (blue)** shows a schematic of the calibration protocol. The prior and posterior PTF parameters are listed in **Suppl. Table S4**.

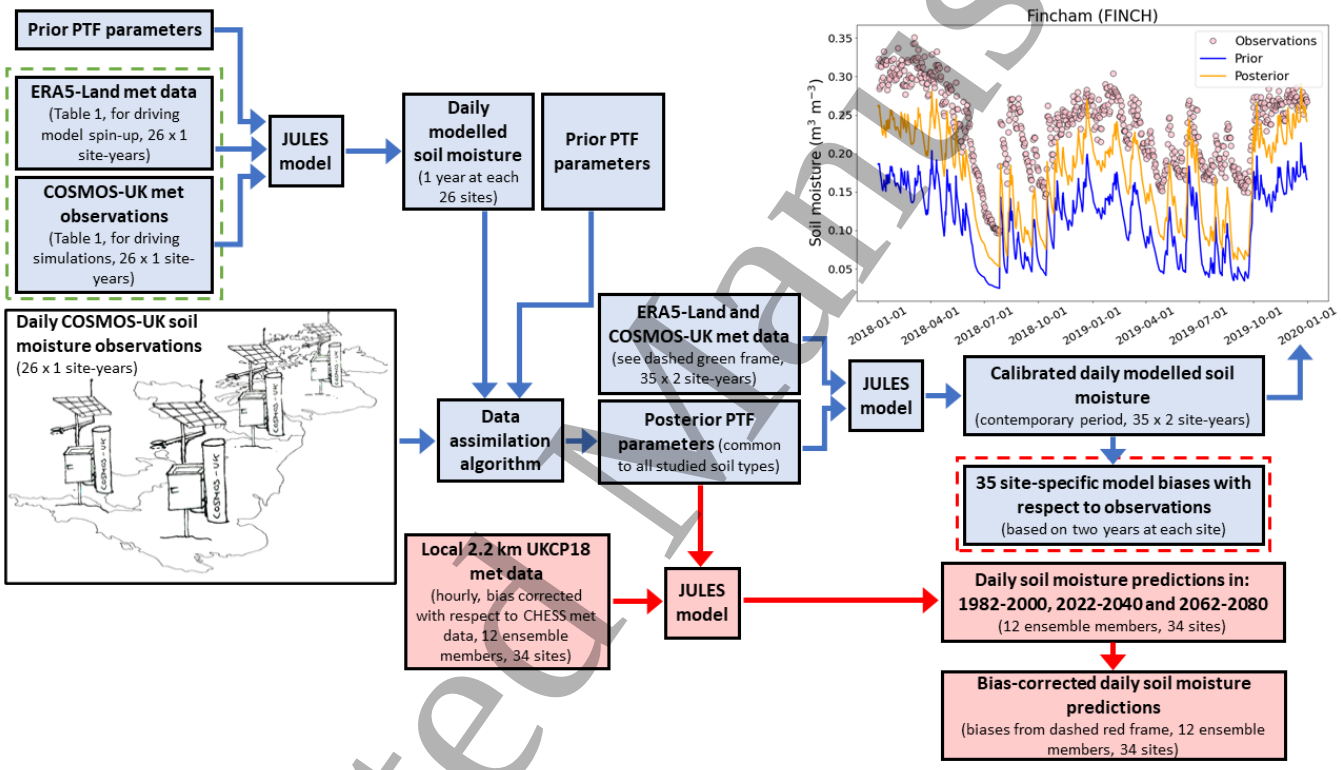

Figure 2. Schematic of the protocol for generating historical and future soil moisture estimates (for periods 1982-2000, 2022-2040 and 2062-2080). Blue boxes indicate stages of the JULES model calibration. Red boxes refer to final future soil moisture predictions given the calibrated JULES model which is forced by UKCP18 data. The top-right panel is an output from JULES, for a representative site (COSMOS-UK code "FINCH"), showing observational data and JULES predictions before and after calibration (i.e. Prior and Posterior respectively). Abbreviation "met" stands for "meteorological" and notation "*a* x *b* site-years" denotes *b* years at each of the *a* sites. We note that while we initially consider 35 sites for the future predictions (blue boxes to the right), in the final analysis (red boxes), we use 34 sites due to the presence of a large soil moisture bias in the modelled data for one of the sites.

2.3.1 JULES model assessment

We assess the modelled soil moisture at all 26 calibration sites and the nine non-calibration sites. We use two continuous years of COSMOS-UK observations, where possible, to compare the measured and modelled daily soil moisture. In the case of calibration sites, this includes the calibration year. We use biases between the modelled output and the observations, and the corresponding unbiased root-mean-square errors as metrics to assess the model **(Suppl. Section S1.6)**. When comparing soil moisture predictions using prior and posterior PTFs to observations, there is an improvement in both metrics for

most of the sites following data assimilation **(Suppl. Table S5)**. For the posterior PTFs, most of the sites show negative soil moisture biases, indicating an overall underestimation of the modelled soil moisture. We note that one of the calibration sites, Lizard (LIZRD), has a very significant model bias and therefore we exclude it from the future soil moisture analysis, leaving 34 sites in total for the future runs.

2.4 Future soil moisture runs with the local 2.2 km UKCP18 data

The local 2.2 km UKCP18 are very high spatial resolution numerical simulations consisting of 12 ensemble members. These simulations are generated by nesting the CPM (HadREM3-GA705) within 12 members of the regional model (HadREM3-RA11M), which is nested within 12 members of the global climate model (HadGEM3-GC3.05). The same CPM structure and parameterisation are used for all 12 simulations of the local UKCP18. However, parameterisations in regional and global models differ between the ensemble members. The ensemble, therefore, captures uncertainties due to alternative parameter values describing the climate system and due to interannual natural variability. The main advantage of the CPM is that it allows the explicit representation of convective storms, resulting in better estimates of the statistical structure of localised, hourly rainfall. The CPM-generated data covers three time periods: 1st December 1980 to 30th November 2000 (1981-2000), 1st December 2020 to 30th November 2040 (2021-2040) and 1st December 2060 to 30th November 2080 (2061-2080). Each modelled month consists of 30 days, and the two future periods follow the high-emissions scenario RCP8.5. We note that new transient simulations have data for periods 2001-2020 and 2041-2060 **(Kendon *et al* 2023)**, but this was not the case during the time of producing the results.

We use the whole ensemble of the local UKCP18 data released in July 2021 with rectified calculations removing earlier errors in the representation of graupel. We select meteorological variables required to drive the JULES model, nearest to the selected stations, and convert them to match the ones in **Table 1 (Suppl. Section S1.8.1)**. We then individually bias correct all 12 ensemble members during the period 1981-2000 using the long-term, observation-based, daily CHESS meteorological data gridded at 1 km resolution **(Robinson *et al* 2020) (Suppl. Section S1.8.2)**. We apply the bias correction to past and future UKCP18 data and ensure that all driving variables are at an hourly resolution **(Suppl. Section S1.8.3)**. The first year of driving data (for each period, site and ensemble member) is used for the calibrated JULES model spin-up and, therefore, is not included in the final analysis. We perform the model spin-up three times and move to the simulation period on 1st January. The remaining years of each period are then used to drive the calibrated JULES model **(Section 2.3)** and produce 12 realisations of daily soil moisture at 34 sites for the three time periods **(Figure 2, red)**. Given the dry model biases **(Suppl. Table S5)** present in the contemporary period, we also consider a second scenario of bias-corrected soil moisture **(Section 2.5.4)**. We note that each of the time periods ends on 29th rather than 30th November due to our model configuration. We use an average of the top two modelled soil moisture layers, up to 35 cm in total, as this approximately corresponds to the CRNS depth. We apply weightings of 10/35 and 25/35 for layers 0-10 cm and 10-35 cm respectively to account for the two different layer thicknesses.

2.5 Data analysis

We analyse the generated soil moisture data in the context of plant water stress (PWS) which we use to identify soil moisture droughts. A plant experiences water stress when the fraction of available water (F_{AW}), accessible via roots, falls below a certain threshold, commonly defined as 0.5 **(Allen *et al* 1998; Grillakis 2019; Hunt *et al* 2009)**. It is based on findings of **(Baier 1969)** which shows that evapotranspiration is soil water-limited below this threshold. We choose this generic threshold for our fixed soil depth as a guide for the future PWS impact. With this, we calculate a daily soil moisture index (SMI) **(Hunt *et al* 2009)** defined as

$$SMI = -5 + 10F_{AW} \qquad \textbf{(1)}$$

and

$$F_{AW} = \frac{\theta - \theta_{WP}}{\theta_{FC} - \theta_{WP}}, \qquad \textbf{(2)}$$

where θ is the soil water content, θ_{FC} is the field capacity (FC) and θ_{WP} is the permanent wilting point (PWP). We define PWP and FC as the soil water contents at a soil matric potential of -1500 kPa and -33 kPa respectively **(Kirkham 2014)**. SMI values decreasing from zero indicate increasing PWS up to PWP (when $F_{AW} = 0$ and so $SMI = -5$). We apply three SMI bands to categorize the intensity of different stress levels **(Table 2)**.

Plant Water Stress Category	SMI range
Less intense/ moderate	$-2 < SMI \leq 0$
High/ severe	$-4 < SMI \leq -2$
Extreme	$SMI \leq -4$

Table 2. Plant water stress categories.

An alternative to the PWS index is a statistical index **(Samaniego *et al* 2013; Sheffield *et al* 2004)** which quantifies drought relative to the climatology of a given location with a recommendation of at least 30 years of

historical data **(Mckee *et al* 1993)**. We choose the PWS index since we have 19 years of historical data, and it directly relates to the agricultural quantity of interest based on FC and PWP parameters obtained from the calibrated JULES model. To address the danger of making our drought predictions overly extreme given the present dry bias, we also consider a second soil moisture scenario with dry biases removed **(Section 2.5.4)**. These two scenarios provide an upper and lower limit for the final drought analysis results.

2.5.1 Soil moisture drought events

We define a soil moisture drought event at a given site as a time interval when SMI is continuously below or equal to zero, allowing positive SMI values for intervals of at most five days after the event starts. Each drought event is characterised by the average SMI value over the event duration and the total duration. Where the average SMI value of an event falls within the SMI range in **Table 2**, the event is assigned the corresponding stress severity category. For instance, if the average SMI value is -3, the event is categorised as a high/ severe drought event. Additionally, we also assign three event duration categories, up to 30 days, between 31 and 90 days, and above 90 days.

2.5.2 Frequency of soil moisture drought events

For each site s, ensemble member k and UKCP18 time period T (1982-2000, 2022-2040 and 2062-2080), we count the number of drought events, n_{T_sk}, of a given category. An average frequency of an event (per year, per site) for each T and k can then be computed as

$$F_{T\_k} = \frac{\sum_s n_{T\_sk}}{N_S N_Y}, \qquad \textbf{(3)}$$

where N_S = 34 is the number of sites and N_Y = 19 is the number of years in a time period T. We note that F_{T_k} can be higher than one because more than one event of a given category can occur within one year. When comparing future F_{T_k} with the past period, we use an absolute frequency difference, D_{T_k}, defined as

$$D_{T\_k} = F_{T\_k} - F_{Past\_k}, \quad \textbf{(4)}$$

where subscript 'Past' refers to the past period 1982-2000. We choose absolute as opposed to relative differences to avoid dividing by very small numbers due to some historical events being rare.

2.5.3 High stress months and their probability

A high stress month is defined as a month with $SMI \leq -2$ **(Table 2)** for a total of at least 16 days in this month.

For each month m (January to December), site s, ensemble member k and time period T, we count the number of high stress months (n_{T_msk}). The probability that a month is classified as a high stress month across all sites, for each T and k is

$$p_{T\_mk} = \frac{\sum_s n_{T\_msk}}{N_S N_Y}. \qquad \textbf{(5)}$$

Similarly to **Eqn. 4**, we use absolute probability differences to compare future p_{T_mk} with the past period,

$$D'_{T\_mk} = p_{T\_mk} - p_{Past\_mk}. \qquad \textbf{(6)}$$

2.5.4 Uncertainty analysis

The metrics of interest in this study are frequency of drought events **(Section 2.5.2, Eqns. 3 and 4)** and probability of high stress months **(Section 2.5.3, Eqns. 5 and 6)**. The corresponding uncertainty analysis considers both climate model and land surface model uncertainties. For the climate model uncertainty, we calculate a given metric for each of the 12 soil moisture simulations which vary due to the variations in the UKCP18 ensemble. We then consider a range between the minimum and maximum values of the resulting 12 metric values. For the land surface model uncertainty, we consider results derived using two scenarios: soil moisture output from the calibrated JULES model (θ') and that same output with biases removed as a post-processing stage after running the model (θ). They are defined as

$$\theta_{T\_sk} = \theta'_{T\_sk} - b_s, \qquad \textbf{(7)}$$

where T is the UKCP18 time period, s is site, k is the ensemble member and b_s is the site-specific model bias calculated in the contemporary period with respect to field-scale soil moisture observations (given in **Suppl. Table S5** and defined in **Eqn. S16** of **Suppl. Section S1.6**). We use the bias-corrected soil moisture scenario alongside the non-bias-corrected version to address how the negative (dry) model bias present at most of the sites may impact our drought conclusions. It provides a more conservative drought analysis given the observations, and we treat both scenarios as feasible. We note that we only bias correct sites with a negative model bias as correcting for positive biases often resulted in unrealistically low soil moisture values in the future. It also further provides a scenario with wetter soils.

Combining soil moisture simulations resulting from the climate model and land surface model uncertainties, we obtain 12 x 2 simulations. Our final results of changes in drought event frequency **(Eqn. 4)** and high stress month probability **(Eqn. 6)** are expressed as the upper and lower limits of the values derived from the 24 simulations.

3 Results

The aggregated future changes in soil moisture and precipitation, with respect to the historical period, are plotted in **Figure 3**. On average, across all 34 sites and 12 ensemble members, a decrease in soil moisture is expected, especially in the summer, late spring and early autumn.

This is consistent with an average decrease in precipitation during this time of year and may also be partly due to an increase in evapotranspiration due to higher temperatures. In the winter, future precipitation is, on average, higher than in the past period which reduces the negative soil moisture changes. The following subsections show how these soil moisture changes affect the frequency of soil moisture drought events and PWS intensity in individual months.

3.1 Frequency of soil moisture drought events

Figure 4 summarises the evolution of soil moisture drought events for different intensity and duration categories, cumulatively across all sites **(Eqn. 3)** and ensemble members. For all three intensity levels (less intense/ moderate, high/ severe and extreme, panels a-c), there is an average decline or a very small increase of the short-term (1-30 days) and medium-term (31-90 days) events in a changed future climate. We note, however, that the uncertainty on this finding is large. Such decreases or very gentle increases can be expected because lower-intensity and shorter-duration events evolve into higher-intensity and longer-duration events under the rising GHGs (scenario RCP8.5). This is shown in **Figure 4c**, where extreme events above 90 days increase significantly in the future. These long-term events will likely spread over most of the driest season replacing medium-duration events. This result is of particular policy concern as under the considered uncertainties **(Section 2.5.4)**, an increase of between 0.1 and 0.6 per year is expected in the frequency of extreme events above 90 days in 2062-2080 **(Table 3)**. This is equivalent to at least two and up to 12 additional events in a 20-year period. When considering the soil moisture scenario with modelled negative biases removed (right-hand bars of **Figure 4c**), such a drought event is expected to occur every 4.5 years.

With the impact implications of long-duration drought conditions likely to be of most interest to climate adaptation planning, we disaggregate geographically the frequency of extreme drought events for durations above 90 days. This is shown in **Figure 5** as the difference between ensemble-average frequencies in periods 2062-2080 and 1982-2000. In the case of soil moisture without bias correction **(Figure 5a)**, 27 sites are projected to have frequency increases above 0.15 per year (equivalent to an extra three events in a 20-year period) in 2062-2080. In the wetter, bias corrected case **(Figure 5b)**, 13 sites show such frequency increases. In the bias corrected scenario, we see that most of the increases occur in the highly populated South East, East of England and East Midlands regions. However, we note that the number of sites in the other regions is relatively small.

3.2 Probability of high stress months

Figure 6 shows probabilities of individual months being classified as high stress months, cumulatively across all sites **(Eqn. 5)** and ensemble members. These probabilities peak in July, August and September for the past and future time periods. Relative to the past period, the risk of high (or more intense) drought conditions increases significantly for months between June and September in 2022-2040 and between May and November in 2062-2080. Here, we only select months where the maximum value of the historical period is lower than the minimum value of a future period. In the far future, of particular concern are months between June and October which see especially significant absolute increases with respect to the considered uncertainties and against a high baseline risk (1982-2000). For the simulations with bias correction, the probability increase for August and September would, on average, lead to high stress months more than every second year increasing the risk of multi-year droughts, and slower recovery of water resources. Months May and November are also alarming as these see large proportional increases, but with respect to a relatively low historical baseline. **Table 3** lists the expected minimum and maximum absolute probability increases between periods 2062-2080 and 1982-2000 for months between May and November.

4 Discussion

Our results project an increased frequency of future long duration, extreme soil moisture drought events. This finding is broadly consistent with other analyses also reporting more severe future soil moisture droughts in the UK **(Grillakis 2019; Kendon *et al* 2019; Rudd *et al* 2019)**, but here with the added benefit of direct knowledge of soil moisture features gained from COSMOS-UK data. Our projected increases in future probabilities of high (or more intense) plant water stress between May and November imply that these months will increasingly experience exceptionally dry soils. Such dry soils in autumn will delay the effect of subsequent wetting days, agreeing with **Kay *et al* (2022)**.

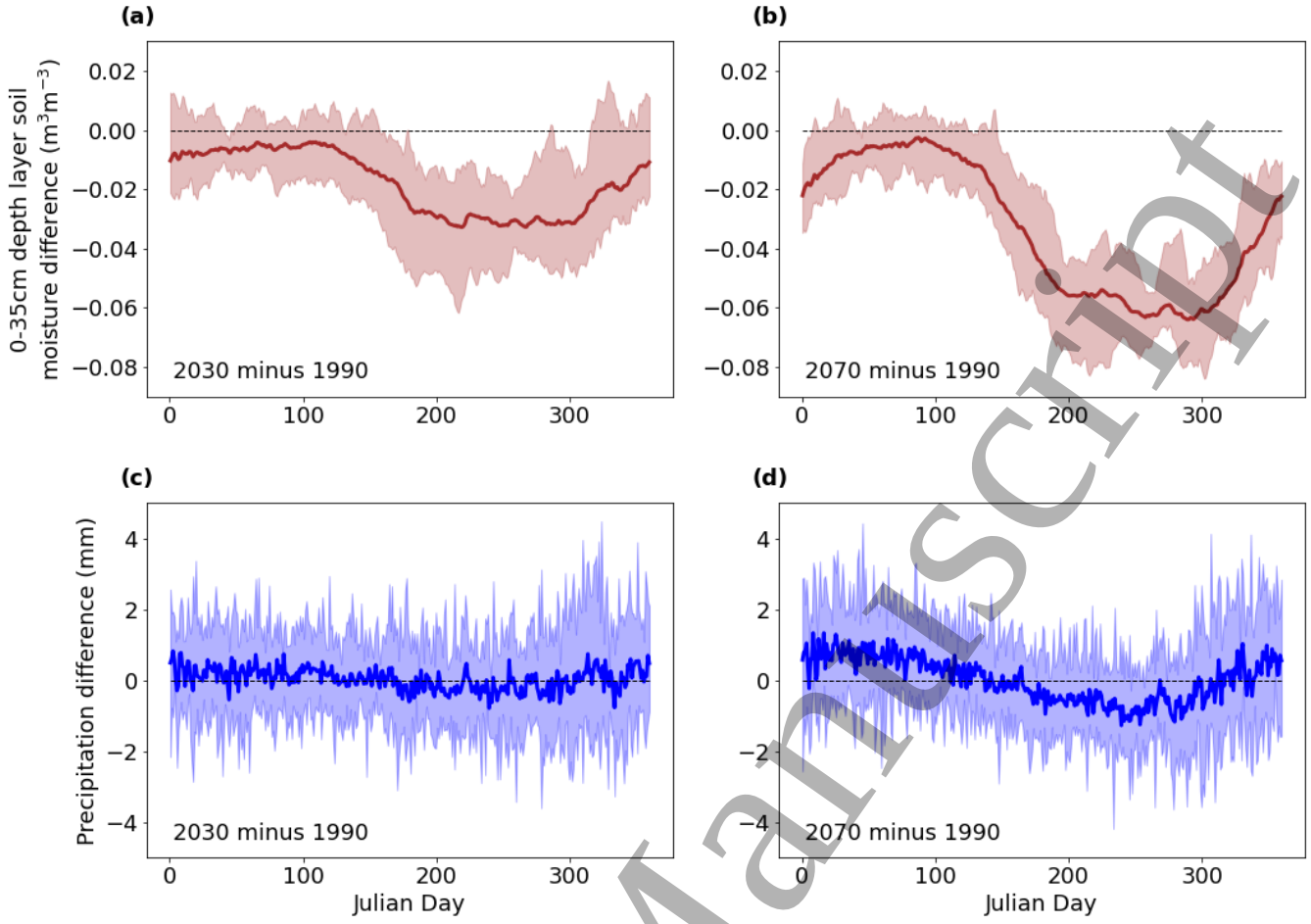

Figure 3. Projected changes in the modelled soil moisture and the UKCP18 precipitation for future time periods, 2022-2040 (labelled as 2030) and 2062-2080 (labelled as 2070). The changes are presented as differences with respect to the past time period 1982-2000 (labelled as 1990). To obtain the plots, for each COSMOS-UK site (Figure 1) and each UKCP18 ensemble member, interannual means (of precipitation or soil moisture) across years of each future time period are calculated, followed by differencing between the future and past time periods. The differences are averaged across all 34 sites and then aggregated across the 12 ensemble members by: averaging (thick continuous lines) and minimising and maximising (spreads of the 12 values for each day). The black horizontal dashed lines mark y-values of zero in each subplot.

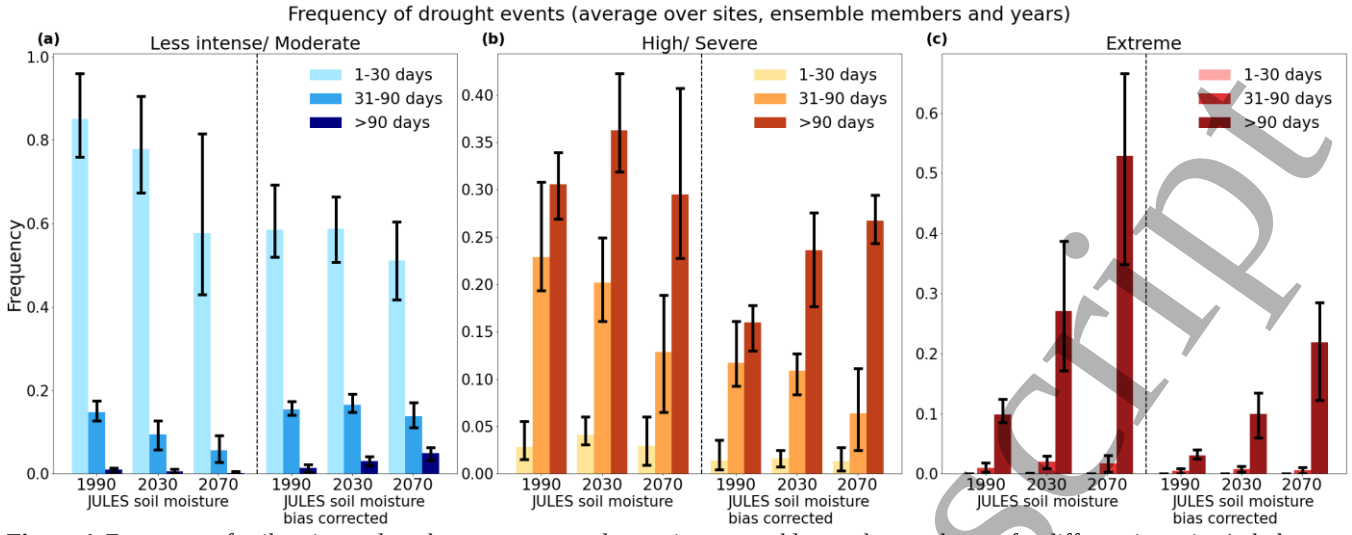

Figure 4. Frequency of soil moisture drought events averaged over sites, ensemble members and years for different intensity (subplots a-c, see Section 2.5.1) and duration regimes (different colour shades). Each subplot contains information for three time periods, 1982-2000 (labelled as 1990), 2022-2040 (labelled as 2030) and 2062-2080 (labelled as 2070) and for three time-durations. The subplots are additionally divided (left or right of vertical dashed line) into two sections which show results derived using modelled soil moisture without (left) and with (right) bias correction. Upper and lower black bars denote the maximum and minimum, respectively, across the UKCP18 ensemble.

Figure 5. Maps showing frequency differences for extreme events (as defined in **Section 2.5.1** and shown in **Figure 4c**) for periods above 90 days. Presented here geographically is the difference between periods 2062-2080 (labelled as 2070) and 1982-2000 (labelled as 1990) for 34 calibrated and predictive calculations at the individual COSMOS-UK sites under study. The differences are averaged across all UKCP18 ensemble members. Maps on the left and right are based on JULES soil moisture without and with bias correction respectively.

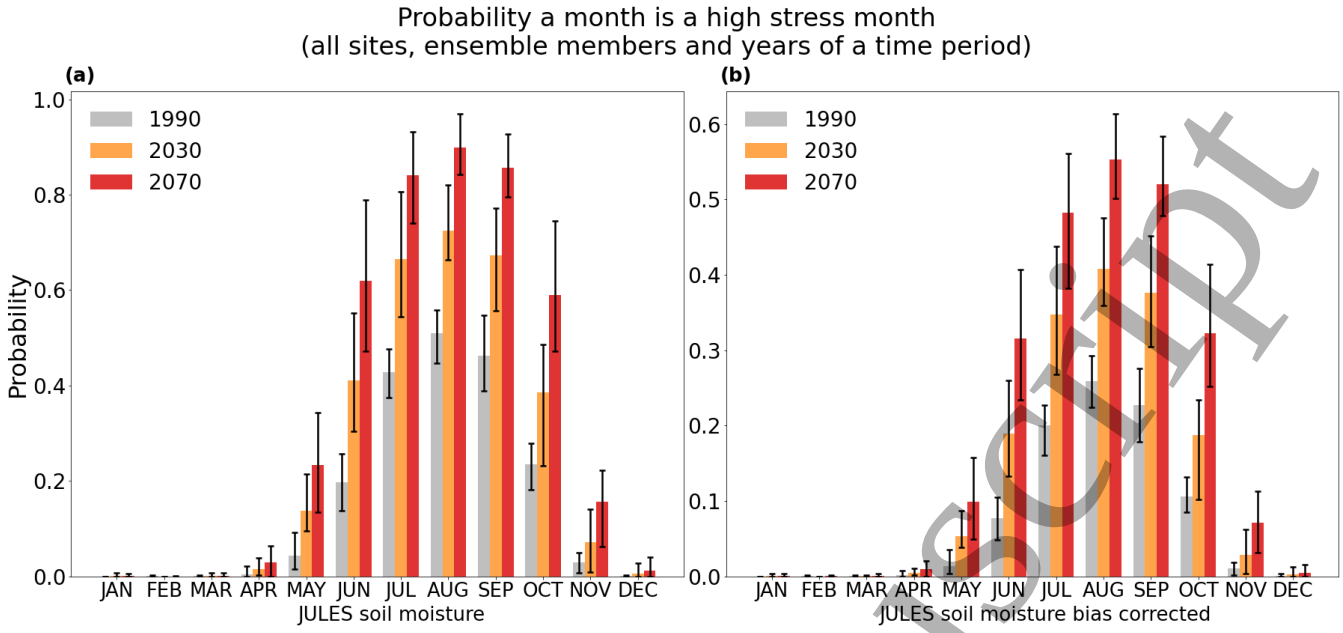

Figure 6. Probability a month is classified as a high stress month across all sites and years of a given time period **(Eqn. 5)**, averaged over the ensemble members. Upper and lower black bars indicate the maximum and minimum across the ensemble respectively. The two subplots correspond to results derived using soil moisture without and with bias correction. Each subplot contains information for three time periods, 1982-2000 (labelled as 1990), 2022-2040 (labelled as 2030) and 2062-2080 (labelled as 2070).

	ABSOLUTE FREQUENCY DIFFERENCE	**ABSOLUTE PROBABILITY DIFFERENCE**						
	Extreme drought events (above 90 days)	**A month is classified as a high stress month**						
		MAY	**JUN**	**JUL**	**AUG**	**SEP**	**OCT**	**NOV**
MINIMUM	0.1	0.04	0.16	0.20	0.25	0.21	0.13	0.02
MAXIMUM	0.6	0.29	0.61	0.53	0.44	0.48	0.51	0.21

Table 3. Temporal comparison of two types of events between time periods 2062-2080 and 1982-2000. The events are frequency of extreme drought events above 90 days (per site, per year) and probability of a selected month being classified as a high stress month (across all sites and years of a time period). The comparison metric is frequency difference **(Eqn. 4)** in the former and probability difference **(Eqn. 6)** in the latter case. The minimum and maximum are calculated based on values obtained from 12 UKCP18 soil moisture simulations with and 12 without bias-correction (24 simulations in total) **(Section 2.5.4)**. Probabilities used to produce probability differences have range between 0 and 1.

Of particular note is the higher autumn stress which will affect autumn sown cereals, for instance winter wheat, at the beginning of their foundation phases, potentially reducing yields. The autumn stress may also lead to the prolongation of water-limited grazing productivity. The drought conditions in the early spring and summer will influence crops in their growing stages. Work in **Slater *et al* (2022)** finds that on average, for broad UK regions, climate change is likely to have beneficial impacts on wheat yields. Nevertheless, the authors highlight that the increased likelihood of prolonged, extreme weather will generate conditions outside of the typical current climatic envelope posing risks to future farming.

Very dry soils will also have a negative impact on grasslands which are important for biodiversity and as grazing resources **(Bengtsson *et al* 2019)**. The dry soils may intensify heatwaves **(Miralles *et al* 2019)** and lead to increasing wildfire risks, especially in the case of highly organic soils and peatlands.

Although our modelling strategy of first optimising the PTF parameters provides an improvement in predictive capability, some features of our reparameterization may

contain compensating errors leading to the modelled soil moisture biases (**Suppl. Table S5**). These biases may partially be due to the provided soil textures which have not been measured at COSMOS-UK sites, but instead sourced from the HWSD. Site-specific geology, which is not considered in our JULES configuration, may also contribute towards the observed soil moisture biases. As an example, some COSMOS-UK sites, especially in southern England, have soils overlaying chalk which if not included in the JULES configuration may lead to significant differences between the modelled and measured soil moisture **(Le Vine *et al* 2016)**.

Another limitation is the length of observational records. We took a very cautious approach, carefully selecting sites and years where precipitation data was mostly complete. We also used two years at each site to assess the JULES model in the contemporary period for each individual location, noting that the test dataset includes one year of training data for the calibration sites. In the future, we hope there will be more long-term and complete datasets to allow non-overlapping and longer timeseries for parameter optimisation and evaluation phases. Further, as the period of record lengthens, it may be possible to use routinely the COSMOS-UK meteorological measurements, instead of CHESS data, for bias correction of climate data. This highlights the importance of maintaining high quality, complete and long-term measurement records.

As noted in **Koster *et al* (2009)**, modelled soil moisture depends not only on model-specific soil parameters, but also on formulations of other water balance variables such as evaporation and runoff. Due to the dependency between water balance variables, data assimilation of soil moisture observations may impact these other variables which then may affect future soil moisture predictions. To that end, comparison against observations for other water balance variables would be ideal, but since we do not have such dataset, we can only assess changes before and after model calibration. We therefore compare evaporation and runoff variables before and after data assimilation for the contemporary period **(Suppl. Section S1.7)**. We find that overall, our data assimilation has a relatively small impact on the timeseries of both variables, especially evaporation, and the JULES-derived values of these two variables appear reasonable. We also note that the risk of compensating errors from other parts of the model affects almost every aspect of simulating climate. That said, even with the risk of compensating errors, the reduction of bias for a strategic state variable such as soil moisture will also in general improve a model's projection of its future value **(Michibata & Suzuki 2020; Zhao *et al* 2022)**. Future work could include running the optimised model at sites where other water balance observations are available, noting here that **Pinnington *et al* (2021)** reports improved sensible and latent heat fluxes when using this method, albeit for a different observation set. Additionally, authors of **Cooper *et al* (2022)** use soil parameters calibrated in this way in gridded JULES runs and evaluate modelled river flow against observations. Their findings show an improvement of modelled river flow for some gauges, but degradation of the output at other sites, so it is not conclusive. Further, an optimisation constraining multiple water balance variables is an active research area in this topic, also suggested as an outlook in **Cooper *et al* (2022)**.

Finally, for the climate model uncertainty, the local UKCP18 data assumes a single, high emissions scenario RCP8.5 and a single structure of the Earth System Model (ESM). The ensemble does, however, capture large-scale uncertainties due to natural climate variability and parametric uncertainties in the driving ESM. The parameters of the local UKCP18 CPM itself are not varied, however, it is an ongoing research at the UK Met Office to sample uncertainties originating from the CPM physics.

5 Conclusions

This study looks at future soil moisture at 34 COSMOS-UK observation sites in two time periods: 1st December 2021 till 29th November 2040 and 1st December 2061 till 29th November 2080, with reference to the past period 1st December 1981 and 29th November 2000. For modelling soil moisture, we first calibrate the JULES model with COSMOS-UK observations and then drive the calibrated model with convection-permitting UKCP18 data. We analyse the results in the context of soil moisture droughts. We define soil moisture drought events according to their maximum plant water stress characteristics: less intense/ moderate, high/ severe and extreme **(Table 2)**, and duration: up to 30 days, between 31 and 90 days, and above 90 days.

On average over the studied sites, we find a significant increase in frequency of extreme drought events above 90 days in both future time periods. This is especially true in 2062-2080, where an increase by a factor between 1.8 and 2.8 is expected with respect to the past period. For individual sites and on average over the UKCP18 ensemble, at least 16 sites show significant increases in the number of these highest severity events in the far future period. Finally, in 2022-2040, an increasing number of months between June and September experience high or more intense stress for at least 16 days. In 2062-2080, this period stretches to between May and November, with months between June and October seeing especially significant increases **(Table 3)**.

Future soil moisture modelling is an active research area **(Seneviratne *et al* 2010)**. Our work is the first case study of future soil moisture predictions based on an observational soil moisture network. It is also a good example of using the CPM data in such modelling framework, with an outlook to expand the analysis to the whole UK, to better determine land impacts under future climate.

Data availability statement

The COMOS-UK data (up to 2022) is available through the Environmental Information Data Centre (EIDC, hosted by

UKCEH) under the Open Government License: COSMOS-UK **(Stanley *et al* 2023)**. The more recent data can be accessed via an API (https://cosmos-api.ceh.ac.uk/docs). The Environment Agency 15-minute rainfall data is available from the Hydrology Data Explorer (https://environment.data.gov.uk/hydrology/doc/reference) under the Open Government Licence 3.0 (https://www.nationalarchives.gov.uk/doc/open-government-licence/version/3/). The 2.2 km Local UKCP18 data is available from the UK Met Office (https://www.metoffice.gov.uk/research/approach/collaboration/ukcp/data/index). The particular version of data we used is from a mirror of the UKCP18 data, accessed in year 2022 and hosted on the JASMIN server. We used the most recent version of the CHESS-Met data, freely available from the EIDC portal (https://catalogue.ceh.ac.uk/documents/2ab15bf0-ad08-415c-ba64-831168be7293). The ERA5-Land hourly data is available from the Copernicus Climate Change Service (C3S) Data Store at https://doi.org/10.24381/cds.e2161bac. JULES source code, instructions for access and running are available from the JULES FCM repository (https://code.metoffice.gov.uk/trac/jules/wiki/WaysToRunJules) which requires registration to access (https://jules-lsm.github.io/). The specific configurations and namelists used to run the experiments in the paper are available at https://code.metoffice.gov.uk/trac/jules with the suite ids: u-ct670 for the optimisation and present-day runs at the calibration sites, u-cw973 for all the future runs and u-cx443 for the present-day runs at the extra sites. The generated modelled soil moisture and bias-corrected UKCP18 data for the considered historical and future time periods are available at https://doi.org/10.5281/zenodo.10645188. Values of leaf area index and canopy height for COSMOS-UK sites are also included there.

Acknowledgments

This work was supported by the Natural Environment Research Council award number NE/R016429/1 as part of the UK-SCAPE programme delivering National Capability. MS undertook most of the analysis and data preparation. CH generated the initial concept of merging UKCP18 outputs with COSMOS-UK data via the JULES model. EC carried out all the JULES runs and performed the data assimilation to optimise soil parameters. JGE led development, collection and interpretation of the COSMOS-UK data. MS created the initial drafts of the manuscript, including the diagrams. All authors contributed to discussions and generating the submitted version of the manuscript and figures.

References

Allen, R. G., Pereira, L. S., Raes, D., & Smith, M. (1998). Chapter 8: ETc under soil water stress conditions. In *Crop evapotranspiration: Guidelines for computing crop water requirements*. FAO.

Baier, W. (1969). Concepts of soil moisture availability and their effect on soil moisture estimates from a meteorological budget. *Agricultural Meteorology*, *6*(3), 165-178. https://doi.org/10.1016/0002-1571(69)90002-8

Bengtsson, J., Bullock, J. M., Egoh, B., Everson, C., Everson, T., O'Connor, T., O'Farrell, P. J., Smith, H. G., & Lindborg, R. (2019). Grasslands-more important for ecosystem services than you might think. *Ecosphere*, *10*(2). https://doi.org/10.1002/ecs2.2582

Best, M. J., Pryor, M., Clark, D. B., Rooney, G. G., Essery, R. L. H., Menard, C. B., Edwards, J. M., Hendry, M. A., Porson, A., Gedney, N., Mercado, L. M., Sitch, S., Blyth, E., Boucher, O., Cox, P. M., Grimmond, C. S. B., & Harding, R. J. (2011). The Joint UK Land Environment Simulator (JULES), model description - Part 1: Energy and water fluxes. *Geoscientific Model Development*, *4*(3), 677-699. https://doi.org/10.5194/gmd-4-677-2011

Bush, M., et al. (2020). The first Met Office Unified Model–JULES Regional Atmosphere and Land configuration, RAL1. *Geosci. Model Dev.*, *13*(4), 1999-2029. https://doi.org/10.5194/gmd-13-1999-2020

Chen, Y., Paschalis, A., Kendon, E., Kim, D., & Onof, C. (2021). Changing Spatial Structure of Summer Heavy Rainfall, Using Convection-Permitting Ensemble. *Geophysical Research Letters*, *48*(3), e2020GL090903. https://doi.org/10.1029/2020GL090903

Christidis, N., McCarthy, M., & Stott, P. A. (2020). The increasing likelihood of temperatures above 30 to 40 °C in the United Kingdom. *Nature Communications*, *11*(1), 3093. https://doi.org/10.1038/s41467-020-16834-0

Cooper, E., Blyth, E., Cooper, H., Ellis, R., Pinnington, E., & Dadson, S. J. (2021). Using data assimilation to optimize pedotransfer functions using field-scale in situ soil moisture observations. *Hydrol. Earth Syst. Sci.*, *25*(5), 2445-2458. https://doi.org/10.5194/hess-25-2445-2021

Cooper, E., Martinez-de la Torre, A., Marthews, T., Ellis, R., Kay, A., Wiggins, M., Dadson, S., Rameshwaran, P., Reynard, N., & Clark, D. (2022). *Improved hydrology for regional environmental prediction*. NERC Open Research Archive https://nora.nerc.ac.uk/id/eprint/533230

Cooper, H. M., et al. (2021). COSMOS-UK: national soil moisture and hydrometeorology data for

environmental science research. *Earth Syst. Sci. Data*, *13*(4), 1737-1757. https://doi.org/10.5194/essd-13-1737-2021

Dai, A. (2011). Drought under global warming: a review. *WIREs Climate Change*, *2*(1), 45-65. https://doi.org/10.1002/wcc.81

Evans, J. G., Ward, H. C., Blake, J. R., Hewitt, E. J., Morrison, R., Fry, M., Ball, L. A., Doughty, L. C., Libre, J. W., Hitt, O. E., Rylett, D., Ellis, R. J., Warwick, A. C., Brooks, M., Parkes, M. A., Wright, G. M. H., Singer, A. C., Boorman, D. B., & Jenkins, A. (2016). Soil water content in southern England derived from a cosmic-ray soil moisture observing system - COSMOS-UK. *Hydrological Processes*, *30*(26), 4987-4999. https://doi.org/10.1002/hyp.10929

Fan, J., McConkey, B., Wang, H., & Janzen, H. (2016). Root distribution by depth for temperate agricultural crops. *Field Crops Research*, *189*, 68-74. https://doi.org/10.1016/j.fcr.2016.02.013

Fischer, G., Nachtergaele, F., Prieler, S., Van Velthuizen, H., Verelst, L., & Wiberg, D. (2008). *Global Agro-ecological Zones Assessment for Agriculture (GAEZ 2008)*. IIASA, Laxenburg, Austria and FAO, Rome, Italy. https://www.fao.org/soils-portal/soil-survey/soil-maps-and-databases/harmonized-world-soil-database-v12/en/

Gavrilescu, M. (2021). Water, Soil, and Plants Interactions in a Threatened Environment. *Water*, *13*(19), 2746. https://www.mdpi.com/2073-4441/13/19/2746

Grillakis, M. G. (2019). Increase in severe and extreme soil moisture droughts for Europe under climate change. *Science of the Total Environment*, *660*, 1245-1255. https://doi.org/10.1016/j.scitotenv.2019.01.001

Hanlon, H. M., Bernie, D., Carigi, G., & Lowe, J. A. (2021). Future changes to high impact weather in the UK. *Climatic Change*, *166*(3), 50. https://doi.org/10.1007/s10584-021-03100-5

Hunt, E. D., Hubbard, K. G., Wilhite, D. A., Arkebauer, T. J., & Dutcher, A. L. (2009). The development and evaluation of a soil moisture index. *International Journal of Climatology*, *29*(5), 747-759. https://doi.org/10.1002/joc.1749

Kay, A. L., Lane, R. A., & Bell, V. A. (2022). Grid-based simulation of soil moisture in the UK: future changes in extremes and wetting and drying dates. *Environmental Research Letters*, *17*(7). https://doi.org/10.1088/1748-9326/ac7a4e

Kendon, E., Fosser, G., Murphy, J., Chan, S., Clark, R., Harris, G., Lock, A., Lowe, J., Martin, G., Pirret, J., Roberts, N., Sanderson, M., & Tucker, S. (2019). *UKCP Convection-permitting model projections: Science report*. Met Office Hadley Centre

Kendon, E., Short, C., Cotterill, D., Pirret, J., Chan, S., & Pope, J. (2023). *UK Climate Projections: UKCP Local (2.2 km) Transient Projections*. Met Office Hadley Centre

Kendon, E., Short, C., Pope, J., Chan, S., Wilkinson, J., Tucker, S., Bett, P., & Harris, G. (2021). *Update to UKCP Local (2.2 km) projections*. Met Office Hadley Centre

Kendon, E. J., Ban, N., Roberts, N. M., Fowler, H. J., Roberts, M. J., Chan, S. C., Evans, J. P., Fosser, G., & Wilkinson, J. M. (2017). Do Convection-Permitting Regional Climate Models Improve Projections of Future Precipitation Change? *Bulletin of the American Meteorological Society*, *98*(1), 79-93. https://doi.org/10.1175/BAMS-D-15-0004.1

Kent, C., Dunstone, N., Tucker, S., Scaife, A. A., Brown, S., Kendon, E. J., Smith, D., McLean, L., & Greenwood, S. (2022). Estimating unprecedented extremes in UK summer daily rainfall. *Environmental Research Letters*, *17*(1), 014041. https://doi.org/10.1088/1748-9326/ac42fb

Kirkham, M. B. (2014). Chapter 10 - Field Capacity, Wilting Point, Available Water, and the Nonlimiting Water Range. In M. B. Kirkham (Ed.), *Principles of Soil and Plant Water Relations (Second Edition)* (pp. 153-170). Academic Press. https://doi.org/10.1016/B978-0-12-420022-7.00010-0

Köhli, M., Schrön, M., Zreda, M., Schmidt, U., Dietrich, P., & Zacharias, S. (2015). Footprint characteristics revised for field-scale soil moisture monitoring with cosmic-ray neutrons. *Water Resources Research*, *51*(7), 5772-5790. https://doi.org/10.1002/2015wr017169

Koster, R. D., Guo, Z., Yang, R., Dirmeyer, P. A., Mitchell, K., & Puma, M. J. (2009). On the Nature of Soil Moisture in Land Surface Models. *Journal of Climate*, *22*(16), 4322-4335. https://doi.org/10.1175/2009JCLI2832.1

Le Vine, N., Butler, A., McIntyre, N., & Jackson, C. (2016). Diagnosing hydrological limitations of a land surface model: application of JULES to a deep-groundwater chalk basin. *Hydrol. Earth Syst. Sci.*, *20*(1), 143-159. https://doi.org/10.5194/hess-20-143-2016

Lowe, J. A., et al. (2018). *UKCP18 Science Overview Report*. Met Office Hadley Centre

Mckee, T. B., Doesken, N. J., & Kleist, J. R. (1993). The Relationship of Drought Frequency and Duration to Time Scales. 8th Conference on Applied Climatology, Anaheim, 179-184.

Met Office. (2022). *Seasonal Assessment - Summer 2022*.

Michibata, T., & Suzuki, K. (2020). Reconciling Compensating Errors Between Precipitation Constraints and the Energy Budget in a Climate Model. *Geophysical Research Letters*, *47*(12), e2020GL088340.

https://doi.org/https://doi.org/10.1029/2020GL088340

Miralles, D. G., Gentine, P., Seneviratne, S. I., & Teuling, A. J. (2019). Land–atmospheric feedbacks during droughts and heatwaves: state of the science and current challenges. *Annals of the New York Academy of Sciences*, *1436*(1), 19-35. https://doi.org/10.1111/nyas.13912

Muñoz Sabater, J. (2019). *ERA5-Land hourly data from 1950 to present.* Copernicus Climate Change Service (C3S) Climate Data Store (CDS), https://doi.org/10.24381/cds.e2161bac (Accessed on 17-Mar-2023)

Pinnington, E., Amezcua, J., Cooper, E., Dadson, S., Ellis, R., Peng, J., Robinson, E., Morrison, R., Osborne, S., & Quaife, T. (2021). Improving soil moisture prediction of a high-resolution land surface model by parameterising pedotransfer functions through assimilation of SMAP satellite data. *Hydrol. Earth Syst. Sci.*, *25*(3), 1617-1641. https://doi.org/10.5194/hess-25-1617-2021

Pinnington, E., Quaife, T., Lawless, A., Williams, K., Arkebauer, T., & Scoby, D. (2020). The Land Variational Ensemble Data Assimilation Framework: LAVENDAR v1.0.0. *Geosci. Model Dev.*, *13*(1), 55-69. https://doi.org/10.5194/gmd-13-55-2020

Robinson, E. L., Blyth, E. M., Clark, D. B., Comyn-Platt, E., & Rudd, A. C. (2020). *Climate hydrology and ecology research support system meteorology dataset for Great Britain (1961-2017) [CHESS-met]*. NERC Environmental Information Data Centre, https://doi.org/10.5285/2ab15bf0-ad08-415c-ba64-831168be7293

Rudd, A. C., Kay, A. L., & Bell, V. A. (2019). National-scale analysis of future river flow and soil moisture droughts: potential changes in drought characteristics. *Climatic Change*, *156*(3), 323-340. https://doi.org/10.1007/s10584-019-02528-0

Samaniego, L., Kumar, R., & Zink, M. (2013). Implications of Parameter Uncertainty on Soil Moisture Drought Analysis in Germany. *Journal of Hydrometeorology*, *14*(1), 47-68. https://doi.org/10.1175/JHM-D-12-075.1

Samaniego, L., Thober, S., Kumar, R., Wanders, N., Rakovec, O., Pan, M., Zink, M., Sheffield, J., Wood, E. F., & Marx, A. (2018). Anthropogenic warming exacerbates European soil moisture droughts. *Nature Climate Change*, *8*(5), 421-426. https://doi.org/10.1038/s41558-018-0138-5

Scott, E. (2022). Impact of climate change and biodiversity loss on food security. *House of Lords Library, In focus*.

Seneviratne, S. I., Corti, T., Davin, E. L., Hirschi, M., Jaeger, E. B., Lehner, I., Orlowsky, B., & Teuling, A. J. (2010). Investigating soil moisture–climate interactions in a changing climate: A review. *Earth-Science Reviews*, *99*(3), 125-161. https://doi.org/10.1016/j.earscirev.2010.02.004

Sheffield, J., Goteti, G., Wen, F., & Wood, E. F. (2004). A simulated soil moisture based drought analysis for the United States. *Journal of Geophysical Research: Atmospheres*, *109*(D24). https://doi.org/10.1029/2004JD005182

Slater, L. J., Huntingford, C., Pywell, R. F., Redhead, J. W., & Kendon, E. J. (2022). Resilience of UK crop yields to compound climate change. *Earth System Dynamics*, *13*(3), 1377-1396. https://doi.org/10.5194/esd-13-1377-2022

Stanley, S., et al. (2023). *Daily and sub-daily hydrometeorological and soil data (2013-2022) [COSMOS-UK]*. NERC EDS Environmental Information Data Centre, https://doi.org/10.5285/5060cc27-0b5b-471b-86eb-71f96da0c80f

Turner, S., Barker, L. J., Hannaford, J., Muchan, K., Parry, S., & Sefton, C. (2021). The 2018/2019 drought in the UK: a hydrological appraisal. *Weather*, *76*(8), 248-253. https://doi.org/10.1002/wea.4003

UKCEH. (2022). *Hydrological Summary for the United Kingdom - August 2022*.

Van Looy, K., Bouma, J., Herbst, M., Koestel, J., Minasny, B., Mishra, U., Montzka, C., Nemes, A., Pachepsky, Y. A., Padarian, J., Schaap, M. G., Toth, B., Verhoef, A., Vanderborght, J., van der Ploeg, M. J., Weihermuller, L., Zacharias, S., Zhang, Y. G., & Vereecken, H. (2017). Pedotransfer Functions in Earth System Science: Challenges and Perspectives. *Reviews of Geophysics*, *55*(4), 1199-1256. https://doi.org/10.1002/2017rg000581

Waller, J. A., García-Pintado, J., Mason, D. C., Dance, S. L., & Nichols, N. K. (2018). Technical note: Assessment of observation quality for data assimilation in flood models. *Hydrol. Earth Syst. Sci.*, *22*(7), 3983-3992. https://doi.org/10.5194/hess-22-3983-2018

Zhao, L., Wang, Y., Zhao, C., Dong, X., & Yung, Y. L. (2022). Compensating Errors in Cloud Radiative and Physical Properties over the Southern Ocean in the CMIP6 Climate Models. *Advances in Atmospheric Sciences*, *39*(12), 2156-2171. https://doi.org/10.1007/s00376-022-2036-z

Zreda, M., Shuttleworth, W. J., Zeng, X., Zweck, C., Desilets, D., Franz, T. E., & Rosolem, R. (2012). COSMOS: the COsmic-ray Soil Moisture Observing System. *Hydrology and Earth System Sciences*, *16*(11), 4079-4099. https://doi.org/10.5194/hess-16-4079-2012